

Enhanced Photoluminescence Quantum Yields through Excimer Formation of Cyclometalated Platinum(II) N-Heterocyclic Carbene Complexes

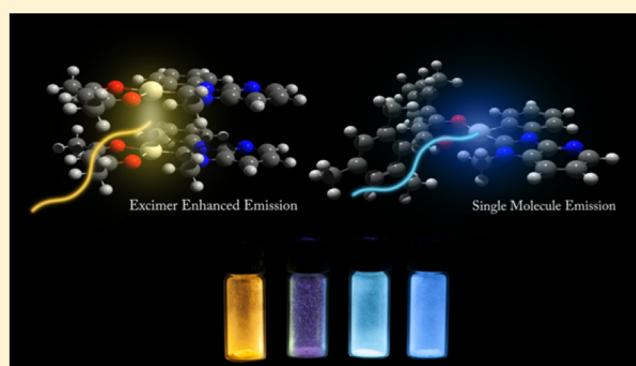
Piermaria Pinter,[†] Hannah Mangold,[‡] Ilona Stengel,[‡] Ingo Münster,[‡] and Thomas Strassner^{*,†}

[†]Professur für Physikalische Organische Chemie, TU Dresden, Bergstrasse 66, 01062 Dresden, Germany

[‡]BASF SE, 67056 Ludwigshafen, Germany

Supporting Information

ABSTRACT: We report a new class of CAC* platinum(II) complexes in which excimer formation enhances the quantum yield while shortening the phosphorescence lifetime. Selective excitation of the monomer or dimer could be achieved at different wavelengths. These complexes exhibit strong phosphorescent emissions in the blue part of the visible spectrum around 450 nm with quantum yields of up to 93%. The emission behavior is controlled through the steric demand of the substituents at the 2,4-pentanedione ligand. We see dual emission with high photoluminescence quantum yields (PLQY) from monomeric and aggregated excited states.

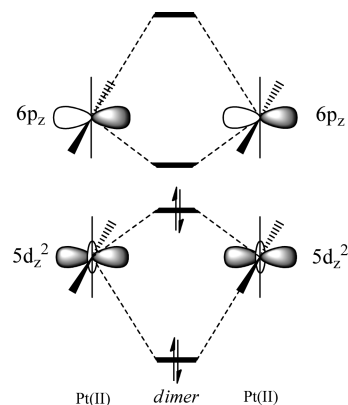


INTRODUCTION

During the past decade, the photophysical properties of platinum complexes have been intensively investigated for their potential use as triplet emitter dopants in OLED devices.^{1–3} We recently reported⁴ complexes of an N-heterocyclic carbene (NHC) in conjunction with a cyclometalated fragment (CAC*) as a very efficient ligand for photophysical applications. The strong σ -donating properties of the CAC* ligand increase the energy gap between occupied and unoccupied orbitals, resulting in a 2-fold desirable effect. An increased energy gap leads to a hypsochromic shift of the emission. In addition, it renders the population of MC (metal-centered) states thermally inaccessible, which are known to deactivate the excited state through radiationless processes.⁵ Moreover, the CAC* moiety allows the precise modification of the electronic properties,^{6–8} while the auxiliary ligand fine-tunes the steric properties,⁹ providing access to a better design of the emitter. Square planar Pt(II) complexes have been known for many years to possess intriguing photophysical and photochemical properties,^{10,11} which to the best of our knowledge were first proposed on the basis of intermolecular interactions in 1971¹² and successively well documented on the basis of excitation dynamics.^{13,14} Depending on the interacting molecular orbital fragments, different intermolecular interactions are possible: π - π stacking derived from ligands with π -systems,¹⁵ π -d interactions between one filled $5d_z^2$ Pt(II) orbital and a π -orbital from a proximal molecule,¹⁶ d-d interactions from the direct interaction of the $5d_z^2$ Pt(II) orbitals,^{11,17–19} or a combination of those.^{20–22} The face-to-face interaction between two Pt(II) atoms splits the z-oriented

$5d_z^2$ (occupied) and $6p_z$ (unoccupied) atomic orbitals to give filled $d\sigma$ and $d\sigma^*$ and unfilled $p\sigma$ and $p\sigma^*$ molecular orbitals, respectively (Scheme 1). At first glance, no Pt–Pt bonding

Scheme 1. Representation of the Face-to-Face Orbital Interaction between Two Pt(II) Atoms

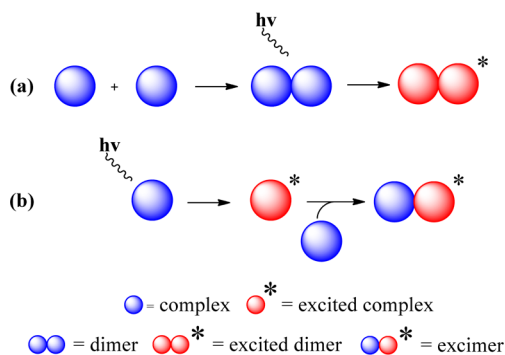


should result as bonding and antibonding orbitals are filled. However, considering configuration interaction, the $d\sigma$ and $d\sigma^*$ orbitals are stabilized while the $p\sigma$ and $p\sigma^*$ orbitals are displaced to higher energies and an overall stabilization occurs; a weak bonding interaction is obtained.^{11,21}

Received: December 2, 2015

These considerations were proven by a time-resolved X-ray diffraction experiment²³ in which a shortening of the Pt–Pt bond of a $[\text{Pt}_2(\text{pop})_4]^{4-}$ complex by 0.28 Å was observed. In accordance with the theoretical model, upon excitation, an electron is promoted from the antibonding $d\sigma^*$ to the weakly bonding $p\sigma$ orbital. Thus, these interactions are strictly dependent on the distance of the interacting orbitals. It has been experimentally^{19,21,24} observed that a distance of 2.9–3.5 Å is sufficient to have a Pt(II)–Pt(II) interaction while for π – π interactions a distance of 3.8 Å has been reported.²⁵ When the intermolecular interactions are negligible, emission originates from an unperturbed single molecule, and for Pt(II) complexes, emissive states ^3LC (ligand-centered), $^3\text{LLCT}$ (ligand-to-ligand charge transfer), or/and $^3\text{MLCT}$ (metal-to-ligand charge transfer)^{26,27} have been characterized. However, when the system allows intermolecular interaction and in particular d–d interaction, a new emissive state arises, namely a $^3\text{MMLCT}$ (metal–metal-to-ligand charge transfer) emissive state.^{10,27} On the basis of theoretical calculations, it has been reported¹⁷ how the d–d interaction underlies the formation of the excimer species, contributing to the lowering of the triplet energy and resulting in a bathochromic shift. Furthermore, a concentration dependency for the formation of the excimer and so for the aggregate emission has been experimentally observed.^{20,28,29} Thus, the bathochromic shift dependent on the concentration of the complex could be ascribed to excimer formation with a new $^3\text{MMLCT}$ emissive state. The formation of the excimers/excited dimers has been proven to follow two pathways:¹³ association of two molecules through intermolecular interactions to form a dimer that is subsequently excited to an excited dimer (Scheme 2a) and excitation of a single molecule followed by formation of an excimer through aggregation with a nonexcited analogue (Scheme 2b).

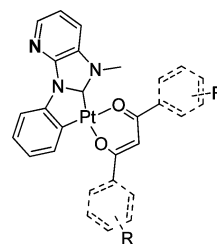
Scheme 2. Representation of the Possible Pathways for Excimer/Excited Dimer Formation



In addition to the self-assembly systems,³⁰ dimeric Pt(II) complexes were obtained using the pyrazolate ligand that could bind two Pt(II) centers in a μ -fashion.²⁴ For this class of complexes, it was found that the degree of interaction depends on the steric demand of the substituents at the pyrazolate.³¹ These unique photophysical properties, in particular, the characteristic dual emissive behavior from single molecules and from excimer, allow one to obtain an extensive choice of emitters and have recently been used to produce efficient WOLEDs.^{19,32–35} A recent report of emissive nanofibers³⁶ showed that at high concentrations the stacked molecules can lead to particular photophysical properties; however, it has usually been experimentally observed^{7,14,37,38} that emission

from aggregates is associated with a lowering of the overall quantum yield due to the self-quenching nature of the excimer. Herein, we report the surprising results of the introduction of a nitrogen atom into the backbone of the NHC moiety³⁹ (Scheme 3), which not only influences the emissive properties

Scheme 3. General Structure of the Reported C \wedge C* Platinum(II) Complexes

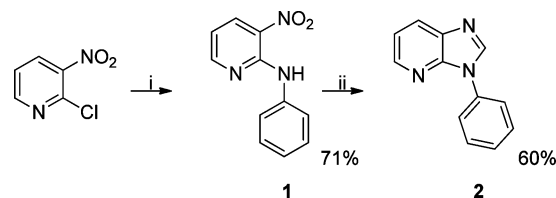


of the complex but also drastically changes the aggregation behavior at low concentrations. Remarkably, the formation of excimers was observed to lower the phosphorescence lifetime without lowering the overall quantum yield; indeed, we report herein an example of an enhanced quantum yield through excimer formation. By the choice of a bulkier acetylacetonate ligand, the stacking could be prevented and only single-molecule emission with excellent photoluminescence properties like quantum yields of up to 93% and a relatively short phosphorescent decay time down to 2.5 μs were observed.

RESULTS AND DISCUSSION

3-Phenyl-3H-imidazo[4,5-*b*]pyridine (**2**) was prepared following a modified two-step procedure⁴⁰ (Scheme 4): synthesis of a

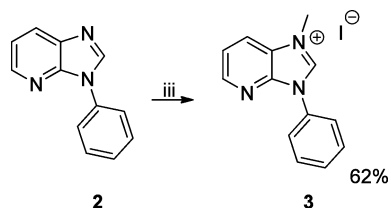
Scheme 4. Synthetic Strategy for the Preparation of the Imidazole Ligand Precursor⁴



^aConditions: (i) *i*-PrOH, base, aniline, reflux for 24 h; (ii) *i*-PrOH, Fe, NH_4Cl , HCOOH, reflux for 48 h.

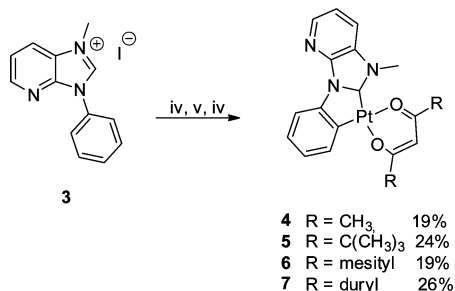
nitro amine derivative through reaction of 2-chloro-3-nitropyridine and aniline in 2-propanol with triethylamine as a base (i), followed by an iron-mediated one-pot reduction of the nitro group and ring closure in formic acid, 2-propanol, and ammonium chloride (ii).

Imidazolium salt (**3**) was obtained through quaternization (iii) with methyl iodide in THF under milder reaction conditions to avoid quaternization at the pyridine nitrogen atom (Scheme 5). Platinum(II) complexes **4–7** were prepared in a one-pot multistep reaction following our recently reported procedure:⁹ formation of the silver(I) NHC complex in DMF through direct deprotonation of the imidazolium salts and formation of the carbene complex with silver(I) oxide (iv), transmetalation of the silver(I) carbene to dichloro(1,5-cyclooctadiene)platinum(II) $[\text{Pt}(\text{COD})\text{Cl}_2]$ (v), and cyclometalation at elevated temperatures followed by reaction with the proper acetylacetonate ligand in the presence of potassium

Scheme 5. Preparation of the Imidazolium Salt^a

^aConditions: (iii) THF, CH₃I, 60 °C, 72 h.

tert-butanolate as a base (vi). Complexes were isolated after column chromatography in 19–26% yields (Scheme 6).

Scheme 6. Synthetic Strategy for the Preparation of the Pt(II) Complexes^a

^aConditions: (iv) DMF, Ag₂O, room temperature to 50 °C; (v) Pt(COD)Cl₂, room temperature to 125 °C; (vi) Hacac, *t*-BuOK, room temperature to 115 °C.

All the complexes were fully characterized by ¹H, ¹³C, and ¹⁹⁵Pt NMR spectroscopy, as well as elemental analysis. The formation of the carbene complex was verified by the disappearance of the characteristic NCHN proton signal of the imidazolium salt in the ¹H NMR experiment. ¹⁹⁵Pt NMR showed a signal in the range of –3349 ppm (5) to –3308 ppm (6), typical for Pt(II) complexes. All complexes are stable at higher temperatures in the range of 257 °C (4) to 297 °C (5). In particular, for complex 7, no decomposition was observed up to a temperature of 350 °C.

Photophysical Properties. The photophysical properties of complexes 4–7 were investigated in amorphous PMMA films at concentrations between 0.2 and 2 wt % at room temperature. UV/vis absorption spectra at 298 K of complexes 4–7 are reported in Figure 1. All complexes show a strong absorption below 255 nm, a weaker shoulder centered at 283 nm, a weak band centered at 305 nm, and a second intense band centered at 330 nm. The transitions are attributed by TD-DFT calculations to the singlet ground state optimized geometry, including a solvent effect with the CPCM⁴¹ model with dichloromethane as the solvent (see Figure 7). The highly energetic absorptions are attributed to a slightly metal perturbed ¹ILCT transition with a small contribution from the diketones;⁹ the transitions centered at 330 nm are attributed to a ¹MLCT state with a major contribution from HOMO–1 → LUMO in agreement with results previously reported.⁹

Via examination of the photoluminescence (PL) spectra (see Figure 2), all complexes show strong phosphorescence at room temperature in the blue region of the spectrum (PL maximum at 456–472 nm) with very good to excellent quantum yields (64–91%) (Table 1). Complex 4 furthermore shows an

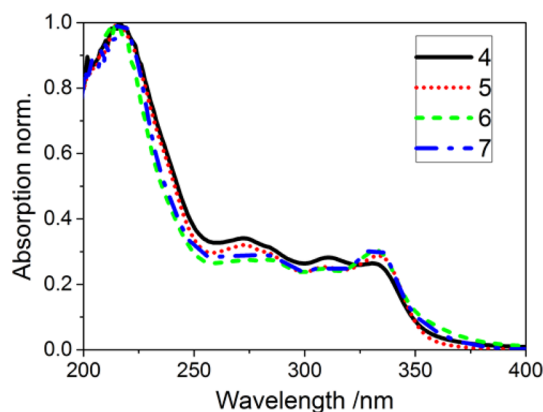


Figure 1. Normalized absorption spectra of complexes 4–7 at room temperature (2 wt % in PMMA).

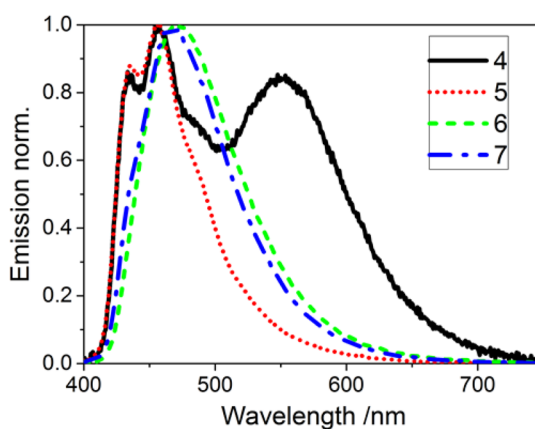


Figure 2. Normalized emission spectra of complexes 4–7 at room temperature (2 wt % in PMMA), with excitation at 340 nm (355 nm for complex 7).

Table 1. Photophysical Data for Complexes 4–7 Measured after Excitation at 340 nm (355 nm for complex 7) under a Nitrogen Atmosphere at Room Temperature for a 2% Film in PMMA and a 100% Film (numbers in parentheses)

	λ_{em} (nm) ^a	ϕ (%) ^c	τ_0 (μ s) ^d	CIE <i>x</i> ; <i>y</i>
4	458; 547 (589), 452 ^b	64 (67)	4.8 (1.4)	0.28; 0.33 (0.51; 0.48)
5	456 (449; 588), 451 ^b	74 (23)	5.8 (1.2)	0.16; 0.13 (0.31; 0.30)
6	472 (497), 452 ^b	91 (41)	2.9 (3.5)	0.18; 0.26 (0.24; 0.43)
7	466 (489), 453 ^b	88 (30)	3.3 (1.8)	0.17; 0.23 (0.22; 0.38)

^aWavelength at the emission maximum. ^bPredicted emission wavelength. ^cQuantum yield. ^dEmissive lifetimes [measured at the emission maximum after excitation with laser pulses (355 nm, 1 ns)] given as $\tau_0 = \tau_v/\phi$ (see Experimental Section).

unstructured band centered around 547 nm as a result of excimer formation, while for complexes with bulkier auxiliary ligands (5–7), no aggregation was observed. Very promising photophysical characteristics were found for complex 6 with a quantum yield of 91% and short emissive decay times of 2.9 μ s.

From the 2% emitter films, it was apparent that the emission and the tendency to aggregate and form excimers differ quite significantly among complexes 4–7. Only complex 4 showed a broad emission centered at 589 nm in addition to the emission in the blue part of the spectrum. On the other hand, the quantum yield remained high for the neat film of complex 4, while it dropped significantly for the other complexes. Upon

close examination of the PL spectra of the neat films of the Pt complexes (see Figure 3), this aggregation behavior is also

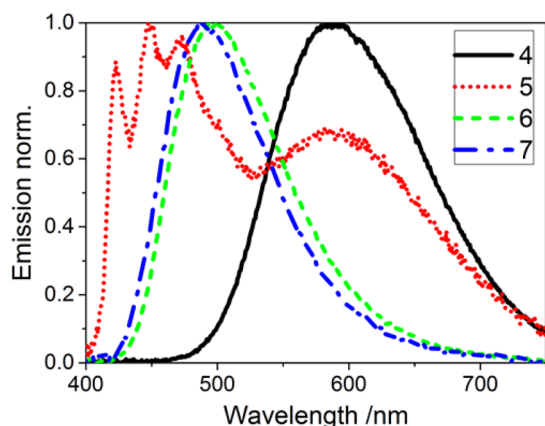


Figure 3. Normalized emission spectra of the 100% film of complexes 4–7 at room temperature (excitation at 340 nm).

apparent. Here complex 4 exhibits only the PL peak of the aggregated species without any contribution of a monomer to the emission. While complexes 6 and 7 show only emission from the monomer, complex 5 exhibits both monomer emission and an additional contribution from an aggregate species with a broad and unstructured peak centered at 588 nm. To understand this aggregation behavior, a series of photoluminescence measurements at different concentrations and with different excitation wavelengths were performed for complexes 4–6, and the results are reported in Table 2.

While the emission of complexes 5 and 6 does not depend on concentration or excitation wavelength, the emission of complex 4 shows a strong dependence on both concentration and excitation wavelength (see Figure 4). Pure single-molecule emission of complex 4 without an excimer contribution is found only at a concentration of 0.2% at an excitation wavelength of 320 or 340 nm. At a concentration of 2%, complex 4 predominantly shows emission from an aggregated species. In the aggregated species of complex 4, the averaged phosphorescence lifetime is reduced by a factor of 2 as a consequence of a new ³MMLCT emissive state. A biexponential global fit of the decay kinetics at both emission maxima and for all three concentrations was conducted to determine the

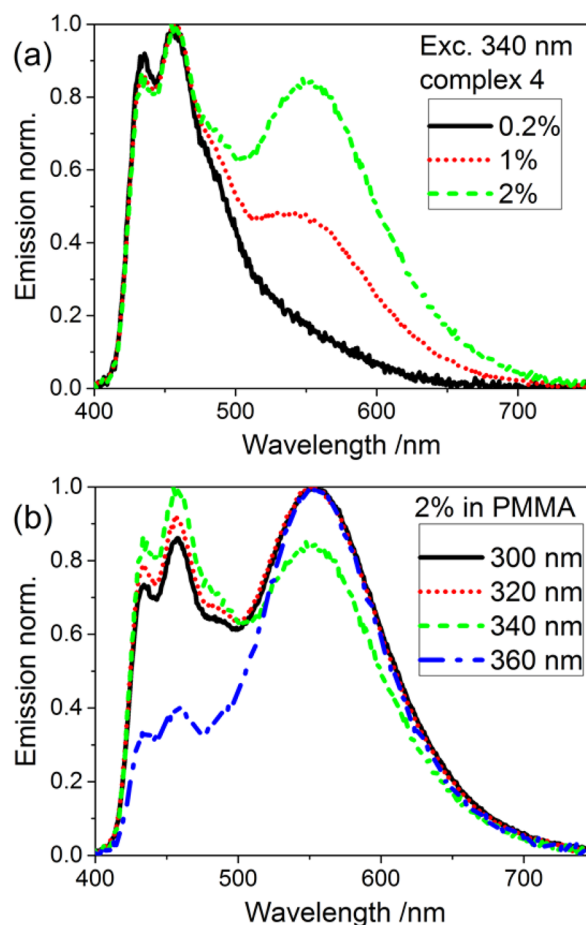


Figure 4. Emission spectra of complex 4 at room temperature (a) at different wt % concentrations in PMMA ($\lambda_{\text{exc}} = 340$ nm) and (b) at different excitation wavelengths at 2 wt % in a PMMA film.

decay constant of the monomer τ_m and the excimer emission τ_e . It was found that the monomer emission decays with a τ_m of 3.57 μs and the excimer emission with a τ_e of 1.26 μs , which means almost 3 times as fast.

To further investigate monomer and excimer emission, excitation spectra were measured for both PL maxima at 457 and 553 nm, and pronounced differences were found (see Figure 5). The excitation spectrum at 553 nm exhibits a red

Table 2. Photophysical Data for Different Concentrations (wt % in PMMA) of Complexes 4–6 under a Nitrogen Atmosphere at Room Temperature^a

complex	concn (%)	λ_{em} (nm) ^b			ϕ^c (%)			τ_0 (μs) ^d		CIE $x; y$		
		320	340	360	320	340	360	457 ^e	550 ^f	320	340	360
4	0.2	456	456	457	57	58	77	5.3	2.2	0.19; 0.18	0.18; 0.16	0.26; 0.31
4	1	457	457	553	64	61	74	4.1	2.1	0.25; 0.29	0.24; 0.26	0.33; 0.42
4	2	552	458	555	67	64	75	4.8	2.1	0.30; 0.36	0.28; 0.33	0.35; 0.45
5	0.2		456			71			5.2		0.15; 0.12	
5	1		456			74			4.6		0.15; 0.13	
5	2		456			74			5.8		0.15; 0.13	
6	0.2		469			93			2.5		0.17; 0.25	
6	1		470			93			2.6		0.17; 0.25	
6	2		472			91			2.9		0.18; 0.26	

^aExcitation at 340 nm for complexes 5 and 6; different excitation wavelengths for complex 4 given in the second line of the table. ^bWavelength at emission maximum. ^cQuantum yield. ^dEmissive lifetimes [excitation with laser pulses (355 nm, 1 ns)] given as $\tau_0 = \tau_v/\phi$. ^eLifetime measured at the maxima of the monomer. ^fLifetime measured at the maxima of the aggregate emission.

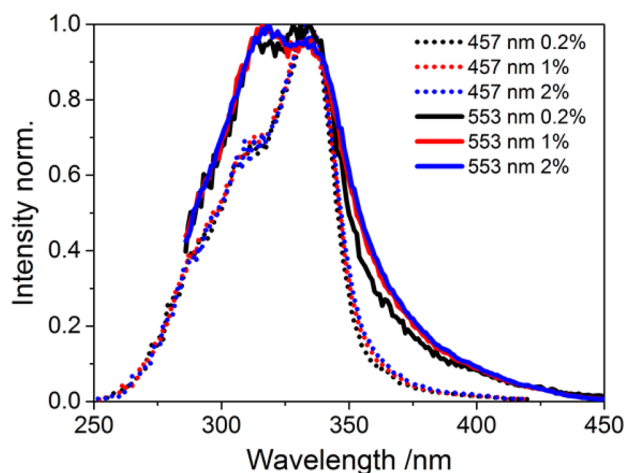


Figure 5. Excitation spectra of complex 4 at room temperature (wt % concentration in PMMA) measured at both emission maxima.

shoulder up to 450 nm compared to the spectrum at 457 nm. This difference explains the excitation wavelength dependence of the PL spectra, especially the more pronounced aggregate peak after excitation at 360 nm compared to excitation at 340 nm.

Surprisingly, the excitation spectra also show a higher intensity around 300–330 nm for the aggregated species. This is further confirmed by the absorption spectra (Figure S1 a), in which a higher relative absorption is found for the 2% film of complex 4 (containing more aggregated species) in this wavelength region. Thus, in addition to common excimer formation¹³ after monomer excitation, aggregated species of complex 4 in the ground state, e.g., dimers, can be excited directly to form an excited dimer.

DFT Calculations. DFT and TD-DFT methods have proven to be useful tools for gaining a better understanding of the excited states^{43,44} of emissive complexes. The ultimate goal is to predict the properties of emitters like emission wavelength, phosphorescent quantum yield, and finally radiative decay time. Thus, DFT and TD-DFT calculations of reported complexes 4–7 were performed with the Gaussian 09 software.⁴⁵ Details of the computational approach are given in Experimental Section. Spin densities are shown in Figure 6. Absorption transitions of complexes 4–7 were calculated using TD-DFT calculations from the optimized singlet state geo-

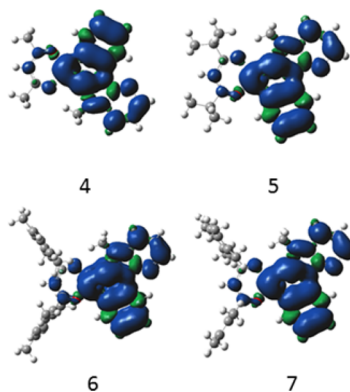


Figure 6. Spin densities calculated at the optimized triplet geometry [B3LYP/6-31G(d)] with Hay-Wadt-ECP (LANL2DZ)^{46,47} for platinum.

metries. The molecular orbital compositions that contribute the most to the transition in the range of 300–330 nm are given in Figure 7. All complexes show an HOMO–1 → LUMO transition, which is attributed to a ¹MLCT process in agreement with previously reported results.⁹

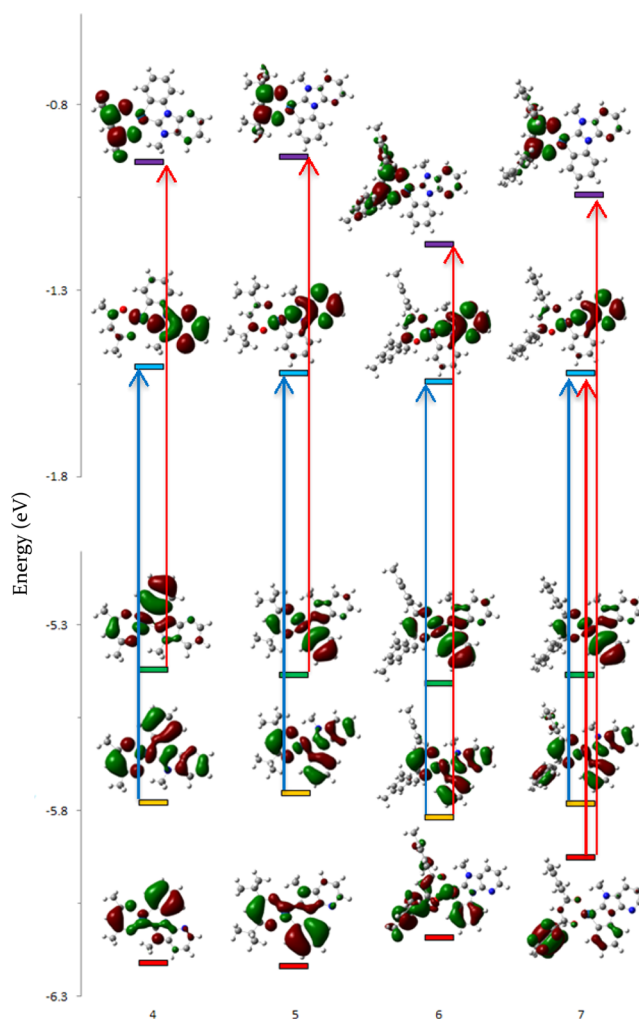


Figure 7. Representation of molecular orbitals involved in the absorption transitions. Orbitals and energies were calculated with TD-DFT methods, and colors are representative of the orbital level involved: red, HOMO–2; yellow, HOMO–1; green, HOMO; blue, LUMO; violet, LUMO+1. The arrows represent the absorption transitions at 304–313 nm (red arrow) and 320–324 nm (blue arrow).

Emission wavelengths were predicted using a method recently reported by our group;⁴² the differences between theory and experiment are in the range of 4–20 nm (values are reported in Table 1). In addition, the spin density of the lowest optimized triplet state was analyzed, and results are reported in Figure 6. The major contributions to the spin density derive from the CAC* fragment and the platinum center with a marginal contribution from the counter ligand. These results underline the separate contributions to the system; the CAC* ligand impacts the electronic properties, while the counter ligand influences the steric properties. In addition to these findings, the plotted spin density resembles a ³ILCT/MLCT emissive state, in accordance with previously reported results.^{9,48}

CONCLUSIONS

We report the synthesis of a new heterocyclic ligand precursor and its first reported use as a CAC* ligand with Pt(II). Four new Pt(II) complexes were characterized, and in particular, the photophysical behavior was studied. Compared to previously studied systems, we discovered that the introduction of a nitrogen into the backbone of the NHC has a drastic influence on both the emissive properties of the complexes and their aggregation behavior. In particular, we have shown that the dual behavior of the system, which is the single molecule and the dimer, could be influenced by the choice of the counter ligand. Bulkier acetylacetonates efficiently prevent molecular aggregation. The imidazopyridine in combination with a sterically demanding counter ligand is found to be an excellent single-molecule emitter with remarkable emissive properties like a quantum yield of 93% and a phosphorescence lifetime of 2.5 μ s at concentrations of 0.2%. Moreover, with the less sterically demanding counter ligand, an unprecedented behavior is observed: excimer formation enhances the quantum yield and shortens the phosphorescence lifetimes by a factor of 3. Furthermore, it was shown that in the case of acetylacetonate, the aggregated species are already present at low complex concentrations, and accordingly, the selective excitation of the monomer or the dimers could be achieved at different wavelengths.

EXPERIMENTAL SECTION

General Experimental Details. DMF was dried according to standard methods and stored over 3 Å molecular sieves under an argon atmosphere. Dichloro(1,5-cyclooctadiene)platinum(II) [Pt(COD)-Cl₂] was prepared following a modified literature procedure.⁴ 1,3-(2,3,5,6-Tetramethylphenyl)propane-1,3-dione and 1,3-(2,4,6-trimethylphenyl)propane-1,3-dione were prepared following reported literature procedures.^{9,49} Potassium tetrachloroplatinate(II) was purchased from Pressure Chemicals Co and used as received. Other chemicals were obtained from common suppliers and were used without further purification. ¹H, ¹³C, and ¹⁹⁵Pt NMR spectra were recorded on a Bruker NMR spectrometer. ¹H and ¹³C spectra were referenced internally using the resonances of the solvent (¹H δ 7.26 and ¹³C δ 77.0 for CDCl₃; ¹H δ 2.50 and ¹³C δ 39.43 for DMSO-*d*₆). ¹⁹⁵Pt spectra were referenced externally using potassium tetrachloroplatinate(II) in D₂O [−1617.2 (PtCl₄^{2−}), −2654.1 (PtCl₂)]. Shifts are given in parts per million downfield from TMS, and coupling constants (*J*) are given in hertz. Elemental analyses were performed by the analytical laboratory of the department using a Eurovektor Hekatech EA-3000 elemental analyzer. Melting points were measured on a hot stage microscope and are not corrected. Photoluminescence measurements were performed in thin PMMA films doped with 0.2, 1, and 2 wt % emitter or from neat emitter films. The films were prepared by doctor blading a solution of emitter in a 10 wt % PMMA solution in dichloromethane on a quartz substrate with a 60 μ m doctor blade. The film was dried, and the emission was measured under nitrogen. Excitation was conducted at wavelengths of 300–360 nm (Xe lamp with a monochromator), and the emission was detected with a calibrated quantum yield detection system (Hamamatsu, model C9920-02). The uncertainty of the quantum yield is \pm 2% for quantum yields of >10%. The phosphorescence decay was measured by excitation with pulses of a THG-NdYAG laser (355 nm, 1 ns) and time-resolved photon counting by a multichannel scaling (MCS) technique. τ_v either is the decay constant obtained from a monoexponential fit or is calculated from a biexponential fit (for decay kinetics that involve both monomer and excimer components) $I(t) = \sum_{i=1}^2 a_i e^{(-t/\tau_i)}$ with the following equation: $\tau_v = (a_1\tau_1^2 + a_2\tau_2^2)/(a_1\tau_1 + a_2\tau_2)$.⁵⁰ From the decay constant τ_v , the emissive decay constant $\tau_0 = \tau_v/(\text{quantum yield})$ is calculated.

The absorption spectra were measured on a Zeiss MCS 601 spectrometer.

Synthesis of Ligands. *3-Nitro-N-phenylpyridin-2-amine (1)*. 2-Chloro-3-nitropyridine (3.0 g, 18.5 mmol), aniline (2.1 g, 22.3 mmol), and triethylamine (2.4 g, 23.3 mmol) were refluxed with 50 mL of 2-propanol for 24 h. Afterward, the reaction mixture was concentrated and extracted with diethyl ether. 3-Nitro-N-phenylpyridine was obtained in 71% yield (2.8 g, 13.2 mmol): ¹H NMR (CDCl₃, 300.13 MHz) δ 10.12 (s, 1H, NH), 8.50 (m, 2H, CH_{arom}), 7.64 (m, 2H, CH_{arom}), 7.42 (m, 2H, CH_{arom}), 7.19 (m, 1H, CH_{arom}), 6.83 (m, 1H, CH_{arom}); ¹³C NMR (CDCl₃, 75.475 MHz) δ 155.4 (CH_{arom}), 150.5 (C_i), 138.0 (C_i), 135.7 (CH_{arom}), 129.2 (CH_{arom}), 128.8 (C_i), 125.0 (CH_{arom}), 122.7 (CH_{arom}), 114.0 (CH_{arom}); mp 60 °C. Anal. Calcd for C₁₁H₉N₃O₂ (215.21 g mol^{−1}): C, 61.39; H, 4.22; N, 19.53. Found: C, 61.54; H, 4.31; N, 19.45.

3-Phenyl-3H-imidazo[4,5-b]pyridine (2). 3-Nitro-N-phenylpyridin-2-amine (1) (10.2 g, 47.4 mmol), formic acid (289 g, 6.3 mol), ammonium chloride (27.1 g, 0.5 mol), and iron powder (70 mesh, 28.3 g, 0.5 mol) were suspended in 200 mL of 2-propanol and refluxed for 48 h. Afterward, the reaction mixture was concentrated to dryness, washed with 200 mL of a saturated aqueous NaHCO₃ solution, and extracted with dichloromethane; organics were dried over MgSO₄, and volatiles were removed. The product was isolated by flash chromatography (silica gel, eluent of ethyl acetate) in 60% yield (5.5 g, 28.3 mmol): ¹H NMR (CDCl₃, 300.13 MHz) δ 8.43 (d, *J* = 4.7 Hz, 1H, CH_{arom}), 8.17 (br, 2H, CH_{arom}), 7.70 (d, *J* = 7.6 Hz, 2H, CH_{arom}), 7.53 (t, *J* = 7.7 Hz, 2H, CH_{arom}), 7.40 (t, *J* = 7.4 Hz, 1H, CH_{arom}), 7.27 (m, 1H, CH_{arom}); ¹³C NMR (CDCl₃, 75.475 MHz) δ 146.9 (C_i), 145.1 (CH_{arom}), 143.1 (CH_{arom}), 136.0 (C_i), 135.2 (C_i), 129.9 (CH_{arom}), 128.5 (CH_{arom}), 128.1 (CH_{arom}), 123.8 (CH_{arom}), 119.1 (CH_{arom}); mp 37 °C. Anal. Calcd for C₁₂H₉N₃ (195.22 g mol^{−1}): C, 73.83; H, 4.65; N, 21.52. Found: C, 73.64; H, 4.72; N, 21.44.

1-Methyl-3-phenyl-3H-imidazo[4,5-b]pyridin-1-ium iodide (3). 3-Phenyl-3H-imidazo[4,5-b]pyridine (2) (2.8 g, 14.4 mmol) and methyl iodide (2.1 g, 14.4 mol) were dissolved in 20 mL of THF and stirred at 60 °C for 72 h in an ACE pressure tube. Afterward, the precipitate was filtered, washed with diethyl ether, and dried *in vacuo*. The product was obtained in 62% yield (3.0 g, 8.9 mmol): ¹H NMR (DMSO-*d*₆, 300.13 MHz) δ 10.41 (s, 1H, NCHN), 8.82 (d, *J* = 4.7 Hz, 1H, CH_{arom}), 8.71 (d, *J* = 7.6 Hz, 1H, CH_{arom}), 7.92 (m, 3H, CH_{arom}), 7.71 (m, 3H, CH_{arom}), 4.21 (s, 3H, CH₃); ¹³C NMR (DMSO-*d*₆, 75.475 MHz) δ 148.6 (CH_{arom}), 144.2 (CH_{arom}), 142.7 (C_i), 132.4 (C_i), 130.1 (CH_{arom}), 129.9 (CH_{arom}), 125.3 (C_i), 125.1 (CH_{arom}), 123.8 (CH_{arom}), 122.5 (CH_{arom}), 34.1 (CH₃); mp 242 °C. Anal. Calcd for C₁₃H₁₂IN₃ (337.16 g mol^{−1}): C, 46.31; H, 3.59; N, 12.46. Found: C, 46.41; H, 3.40; N, 12.51.

Synthesis of Complexes. *(SP-4-3)-[1-Methyl-3-phenyl-imidazo[4,5-b]pyridine-κC2,κC2']-[2,4-pentanedionato-κO2,κO4] Platinum(III) (4)*. A flame-dried and argon-flushed Schlenk tube was charged with 1-methyl-3-phenyl-3H-imidazo[4,5-b]pyridin-1-ium iodide (3) (602 mg, 1.8 mmol) and silver(I) oxide (210 mg, 0.9 mmol). After addition of 50 mL of dry DMF, the reaction mixture was stirred under argon protected from light for 1 h at room temperature and then for 25 h at 50 °C. Dichloro(1,5-cyclooctadiene)platinum(II) (662 mg, 1.8 mmol) was added, and the mixture was stirred for 2 h at 50 °C and then for 30 h at 125 °C. Afterward, potassium *tert*-butanolate (401 mg, 3.6 mmol) and acetylacetonate (368 mg, 3.7 mmol) were added, and the mixture was stirred for 24 h at room temperature and then for 24 h at 115 °C; all volatiles were removed *in vacuo*, and the crude product was washed with water and isolated by flash chromatography (silica gel, eluent of ethyl acetate/iso-hexanes) in 19% yield (166 mg, 0.3 mmol): ¹H NMR (CDCl₃, 300.13 MHz) δ 8.40 (d, *J* = 4.9 Hz, 1H, CH_{arom}), 8.25 (d, *J* = 7.7 Hz, 1H, CH_{arom}), 7.81 (pseudo-t, *J* = 6.0 Hz, *J*_{H,Pt} = 27.0 Hz, 1H, PtCCH_{arom}), 7.60 (d, *J* = 8.0 Hz, 1H, CH_{arom}), 7.22 (m, 1H, CH_{arom}), 7.14 (t, *J* = 7.5 Hz, 1H, CH_{arom}), 7.04 (t, *J* = 7.4 Hz, 1H, CH_{arom}), 5.50 (s, 1H, OCCH), 4.17 (s, 3H, NCH₃), 2.08 (s, 3H, CH₃), 1.99 (s, 3H, CH₃); ¹³C NMR (CDCl₃, 75.475 MHz) δ 185.5 (CO), 185.2 (CO), 163.0 (NC_{NHC}N), 147.1 (C_i), 145.3 (C_i), 144.5 (CH_{arom}), 131.0 (CH_{arom}), 128.4 (C_i), 124.7 (C_i), 124.2 (CH_{arom}), 124.0 (CH_{arom}), 117.9 (CH_{arom}), 117.5 (CH_{arom}), 114.0 (CH_{arom}),

102.2 (CH), 31.6 (NCH₃), 28.1 (CH₃), 28.0 (CH₃); ¹⁹⁵Pt NMR (CDCl₃, 64.51 MHz) δ -3335.89; mp 257 °C. Anal. Calcd for C₁₈H₁₇N₃O₂Pt (502.43 g mol⁻¹): C, 43.03; H, 3.41; N, 8.36. Found: C, 42.66; H, 3.33; N, 8.32.

(*SP-4-3*)-[1-Methyl-3-phenyl-imidazol-2-yliden[4,5-*b*]pyridine- κ C2, κ C2'](*dipivaloylmethanato- κ O2, κ O4*) Platinum(II) (5). A flame-dried and argon-flushed Schlenk tube was charged with 1-methyl-3-phenyl-3*H*-imidazo[4,5-*b*]pyridin-1-ium iodide (3) (350 mg, 1.0 mmol) and silver(I) oxide (122 mg, 0.5 mmol). After addition of 20 mL of dry DMF, the reaction mixture was stirred under argon protected from light for 1 h at room temperature and then for 25 h at 50 °C. Dichloro(1,5-cyclooctadiene)platinum(II) (384 mg, 1.0 mmol) was added, and the mixture was stirred for 2 h at 50 °C and then for 24 h at 125 °C. Afterward, potassium *tert*-butanolate (240 mg, 2.1 mmol) and dipivaloylmethane (393 mg, 2.1 mmol) were added. After the mixture was stirred for 24 h at room temperature followed by 24 h at 115 °C, all volatiles were removed under reduced pressure, and then the crude product was washed with water and isolated by flash chromatography (silica gel, eluent of dichloromethane) in 24% yield (145 mg, 0.2 mmol): ¹H NMR (CDCl₃, 500 MHz) δ 8.43 (d, *J* = 4.9 Hz, 1H, CH_{arom}), 8.31 (d, *J* = 7.5 Hz, 1H, CH_{arom}), 7.92 (pseudo-t, *J* = 7.5 Hz, *J*_{H,Pt} = 24.0 Hz, 1H, PtCCH_{arom}), 7.64 (d, *J* = 8.0 Hz, 1H, CH_{arom}), 7.25 (m, 1H, CH_{arom}), 7.17 (td, *J* = 5.0, 1.0 Hz, 1H, CH_{arom}), 7.04 (td, *J* = 7.5, 1 Hz, 1H, CH_{arom}), 5.90 (s, 1H, OCCH), 4.31 (s, 3H, NCH₃), 1.32 [s, 9H, (CH₃)₃], 1.26 [s, 9H, (CH₃)₃]; ¹³C NMR (CDCl₃, 75.475 MHz) δ 195.5 (CO), 194.9 (CO), 163.7 (NC_{NHCN}), 147.0 (C_i), 145.3 (C_i), 144.6 (CH_{arom}), 131.3 (CH_{arom}), 128.3 (C_i), 124.9 (C_i), 124.2 (CH_{arom}), 124.1 (CH_{arom}), 118.0 (CH_{arom}), 117.5 (CH_{arom}), 114.0 (CH_{arom}), 93.0 (CH), 42.2 [C(CH₃)₃], 41.5 [C(CH₃)₃], 32.1 (NCH₃), 28.9 (CH₃), 28.8 (CH₃); ¹⁹⁵Pt NMR (CDCl₃, 64.51 MHz) δ -3348.63; mp 297 °C. Anal. Calcd for C₂₄H₂₉N₃O₂Pt (586.59 g mol⁻¹): C, 49.14; H, 4.98; N, 7.16. Found: C, 49.45; H, 5.19; N, 7.06.

(*SP-4-3*)-[1-Methyl-3-phenyl-imidazol-2-yliden[4,5-*b*]pyridine- κ C2, κ C2'](*dimesitylmethanato- κ O2, κ O4*) Platinum(II) (6). A flame-dried and argon-flushed Schlenk tube was charged with 1-methyl-3-phenyl-3*H*-imidazo[4,5-*b*]pyridin-1-ium iodide (3) (602 mg, 1.8 mmol) and silver(I) oxide (210 mg, 0.9 mmol). After addition of 50 mL of dry DMF, the reaction mixture was stirred under argon protected from light for 1 h at room temperature and then for 25 h at 50 °C. Dichloro(1,5-cyclooctadiene)platinum(II) (662 mg, 1.8 mmol) was added, and the mixture was stirred for 2 h at 50 °C and then for 30 h at 125 °C. Afterward, potassium *tert*-butanolate (401 mg, 3.6 mmol) and 1,3-(2,4,6-trimethylphenyl)propane-1,3-dione (368 mg, 3.7 mmol) were added, and the mixture was stirred for 24 h at room temperature followed by 24 h at 115 °C; all volatiles were removed under reduced pressure, and then the crude product was washed with water and isolated by flash chromatography (silica gel, eluent of ethyl acetate/iso-hexanes) in 19% yield (166 mg, 0.3 mmol): ¹H NMR (CDCl₃, 300.13 MHz) δ 8.46 (d, *J* = 4.9 Hz, 1H, CH_{arom}), 8.32 (d, *J* = 7.8 Hz, 1H, CH_{arom}), 7.78 (pseudo-t, *J* = 7.5 Hz, *J*_{H,Pt} = 25.2 Hz, 1H, PtCCH_{arom}), 7.65 (d, *J* = 8.1 Hz, 1H, CH_{arom}), 7.26 (m, 1H, CH_{arom}), 7.16 (t, *J* = 7.6 Hz, 1H, CH_{arom}), 7.00 (t, *J* = 7.5 Hz, 1H, CH_{arom}), 6.87 (d, *J* = 7.2 Hz, 4H, CH_{mes}), 5.74 (s, 1H, OCCH), 4.17 (s, 3H, NCH₃), 2.33 [m, 18H, (CH₃)_{mes}]; ¹³C NMR (CDCl₃, 75.475 MHz) δ 185.6 (CO), 185.1 (CO), 162.8 (NC_{NHCN}), 147.0 (C_i), 145.2 (C_i), 144.8 (CH_{arom}), 139.8 (C_i), 139.2 (C_i), 137.9 (C_i), 137.7 (C_i), 134.4 (C_i), 133.9 (C_i), 131.5 (CH_{arom}), 128.4 (CH_{arom}), 128.3 (C_i), 128.2 (CH_{arom}), 124.5 (CH_{arom}), 124.2 (CH_{arom}), 124.1 (C_i), 118.1 (CH_{arom}), 117.6 (CH_{arom}), 114.2 (CH_{arom}), 107.3 (CH), 31.8 (NCH₃), 21.3 [(CH₃)_{mes}], 19.7 [(CH₃)_{mes}]; ¹⁹⁵Pt NMR (CDCl₃, 64.51 MHz) δ -3308.11; mp 289 °C. Anal. Calcd for C₃₄H₃₃N₃O₂Pt (710.73 g mol⁻¹): C, 57.46; H, 4.68; N, 5.91. Found: C, 57.66; H, 4.89; N, 5.87.

(*SP-4-3*)-[1-Methyl-3-phenyl-3*H*-imidazol-2-yliden[4,5-*b*]pyridine- κ C2, κ C2'](*1,3-bis(2,3,5,6-tetramethylphenyl)propane-1,3-dionato- κ O2, κ O4*) Platinum(II) (7). A flame-dried and argon-flushed Schlenk tube was charged with 1-methyl-3-phenyl-3*H*-imidazo[4,5-*b*]pyridin-1-ium iodide (3) (200 mg, 0.6 mmol) and silver(I) oxide (69 mg, 0.3 mmol). After addition of 20 mL of dry DMF, the reaction

mixture was stirred under argon protected from light for 1 h at room temperature and then for 23 h at 60 °C. Dichloro(1,5-cyclooctadiene)platinum(II) (220 mg, 0.6 mmol) was added, and the mixture was stirred for 1 h at 75 °C and then for 22 h at 115 °C. Afterward, potassium *tert*-butanolate (267 mg, 3.6 mmol) and 1,3-(2,3,5,6-tetramethylphenyl)propane-1,3-dione (600 mg, 1.8 mmol) were added, and the mixture was stirred for 10 h at room temperature, then for 6 h at 55 °C, and then for 20 h at 110 °C. All volatiles were removed under reduced pressure, and the crude product was washed with water and isolated by flash chromatography (silica gel, eluent of ethyl acetate/iso-hexanes) in 26% yield (115 mg, 0.2 mmol): ¹H NMR (CDCl₃, 300.13 MHz) δ 8.46 (d, *J* = 4.9 Hz, 1H, CH_{arom}), 8.33 (d, *J* = 7.8 Hz, 1H, CH_{arom}), 7.79 (pseudo-t, *J* = 7.5 Hz, *J*_{H,Pt} = 22.8 Hz, 1H, PtCCH_{arom}), 7.65 (d, *J* = 7.0 Hz, 1H, CH_{arom}), 7.33 (m, 1H, CH_{arom}), 7.19 (t, *J* = 7.6 Hz, 1H, CH_{arom}), 7.02 (m, *J* = 7.5 Hz, 3H, CH_{arom}), 5.70 (s, 1H, OCCH), 4.19 (s, 3H, NCH₃), 2.25 [m, 24H, (CH₃)_{dur}]; ¹³C NMR (CDCl₃, 75.475 MHz) δ 186.5 (CO), 186.1 (CO), 162.7 (NC_{NHCN}), 146.9 (C_i), 145.1 (C_i), 144.7 (CH_{arom}), 142.6 (C_i), 142.2 (C_i), 134.1 (C_i), 133.8 (C_i), 131.5 (CH_{arom}), 131.2 (CH_{arom}), 131.0 (CH_{arom}), 130.5 (C_i), 129.8 (C_i), 129.5 (C_i), 128.2 (C_i), 124.4 (CH_{arom}), 124.0 (CH_{arom}), 117.9 (CH_{arom}), 117.4 (CH_{arom}), 114.0 (CH_{arom}), 107.7 (CH), 31.8 (NCH₃), 19.8 [(CH₃)_{dur}], 19.7 [(CH₃)_{dur}], 16.6 [(CH₃)_{dur}], 16.1 [(CH₃)_{dur}]; ¹⁹⁵Pt NMR (CDCl₃, 64.51 MHz) δ -3316.10; mp >350 °C (no decomposition was observed). Anal. Calcd for C₃₆H₃₇N₃O₂Pt (738.78 g mol⁻¹): C, 58.53; H, 5.05; N, 5.69. Found: C, 58.20; H, 5.07; N, 5.53.

Computational Details. All calculations were performed with Gaussian 09.⁴⁵ The singlet and triplet ground state geometries were optimized using the density functional hybrid model B3LYP^{51–55} together with the 6-31G(d)^{56–61} basis set and the Hay-Wadt-ECP (LANL2DZ)^{46,47} for platinum. All reported intermediates were verified as true minima by the absence of negative eigenvalues in the vibrational frequency analysis. Frontier molecular orbitals were computed on the singlet ground state structure, while the spin densities were calculated on the basis of the ground state structure of the optimized triplet state. Absorption transitions were assigned by TD-DFT at the same level of theory. The first 20 excitations from the optimized singlet state geometries of complexes 4–7 were calculated without spin restriction and the CPCM⁴¹ model (with dichloromethane as the solvent). For visualization, GaussView⁶² was used.

■ ASSOCIATED CONTENT

● Supporting Information

The Supporting Information is available free of charge on the ACS Publications website at DOI: 10.1021/acs.organomet.5b00982.

CIF files, absorption and photoluminescence spectra, PL decay kinetics, and detailed NMR spectra for the optimized structures (PDF)

Cartesian coordinates for the optimized structures (XYZ)

■ AUTHOR INFORMATION

Corresponding Author

*Fax: 49 351 46339679. Telephone: 49 351 46338571. E-mail: thomas.strassner@chemie.tu-dresden.de.

Notes

The authors declare no competing financial interest.

■ ACKNOWLEDGMENTS

We are grateful for the support of the project by the BMBF (FKZ, 13N10477) and thank Dr. Wagenblast and Dr. Lennartz (BASF) for helpful discussions. We also thank the ZIH at the TU Dresden for computation time at their high-performance computing facility.

REFERENCES

- (1) Vezzu, D. A. K.; Deaton, J. C.; Jones, J. S.; Bartolotti, L.; Harris, C. F.; Marchetti, A. P.; Kondakova, M.; Pike, R. D.; Huo, S. *Inorg. Chem.* **2010**, *49*, 5107–5119.
- (2) Williams, J. A. G.; Develay, S.; Rochester, D. L.; Murphy, L. *Coord. Chem. Rev.* **2008**, *252*, 2596–2611.
- (3) Zhou, G.; Wang, Q.; Wang, X.; Ho, C. L.; Wong, W. Y.; Ma, D.; Wang, L.; Lin, Z. *J. Mater. Chem.* **2010**, *20*, 7472–7484.
- (4) Unger, Y.; Meyer, D.; Molt, O.; Schildknecht, C.; Münster, I.; Wagenblast, G.; Strassner, T. *Angew. Chem., Int. Ed.* **2010**, *49*, 10214–10216.
- (5) Chi, Y.; Chou, P. T. *Chem. Soc. Rev.* **2010**, *39*, 638–655.
- (6) Tronnier, A.; Rislér, A.; Langer, N.; Wagenblast, G.; Münster, I.; Strassner, T. *Organometallics* **2012**, *31*, 7447–7452.
- (7) Tronnier, A.; Wagenblast, G.; Münster, I.; Strassner, T. *Chem. - Eur. J.* **2015**, *21*, 12881–12884.
- (8) Tronnier, A.; Pöthig, A.; Metz, S.; Wagenblast, G.; Münster, I.; Strassner, T. *Inorg. Chem.* **2014**, *53*, 6346–6356.
- (9) Tronnier, A.; Heinemeyer, U.; Metz, S.; Wagenblast, G.; Münster, I.; Strassner, T. *J. Mater. Chem. C* **2015**, *3*, 1680–1693.
- (10) Houlding, V. H.; Miskowski, V. M. *Coord. Chem. Rev.* **1991**, *111*, 145–152.
- (11) Krogmann, K. *Angew. Chem., Int. Ed. Engl.* **1969**, *8*, 35–42.
- (12) Martin, D. S. J.; Hunter, L. D.; Kroening, R.; Coley, R. F. *J. Am. Chem. Soc.* **1971**, *93*, 5433–5440.
- (13) Ma, B.; Djurovich, P. I.; Thompson, M. E. *Coord. Chem. Rev.* **2005**, *249*, 1501–1510.
- (14) D'Andrade, B.; Forrest, S. R. *Chem. Phys.* **2003**, *286*, 321–335.
- (15) Miskowski, V. M.; Houlding, V. H. *Inorg. Chem.* **1989**, *28*, 1529–1533.
- (16) Delahaye, S.; Loosli, C.; Liu, S. X.; Decurtins, S.; Labat, G.; Neels, A.; Loosli, A.; Ward, T. R.; Hauser, A. *Adv. Funct. Mater.* **2006**, *16*, 286–295.
- (17) Kim, D.; Bredas, J. L. *J. Am. Chem. Soc.* **2009**, *131*, 11371–11380.
- (18) Büchner, R.; Cunningham, C. T.; Field, J. S.; Haines, R. J.; McMillin, D. R.; Summerton, G. C. *J. Chem. Soc., Dalton Trans.* **1999**, 711–717.
- (19) Ma, B.; Djurovich, P. I.; Garon, S.; Alleyne, B.; Thompson, M. E. *Adv. Funct. Mater.* **2006**, *16*, 2438–2446.
- (20) Bailey, J. A.; Hill, M. G.; Marsh, R. E.; Miskowski, V. M.; Schaefer, W. P.; Gray, H. B. *Inorg. Chem.* **1995**, *34*, 4591–4599.
- (21) Connick, W. B.; Marsh, R. E.; Schaefer, W. P.; Gray, H. B. *Inorg. Chem.* **1997**, *36*, 913–922.
- (22) Stengel, I.; Strassert, C. A.; De Cola, L.; Bäuerle, P. *Organometallics* **2014**, *33*, 1345–1355.
- (23) Kim, C. D.; Pillet, S.; Wu, G.; Fullagar, K.; Coppens, P. *Acta Crystallogr., Sect. A: Found. Crystallogr.* **2002**, *58*, 133–137.
- (24) Ma, B.; Li, J.; Djurovich, P. I.; Yousufuddin, M.; Bau, R.; Thompson, M. E. *J. Am. Chem. Soc.* **2005**, *127*, 28–29.
- (25) Hunter, C. A.; Sanders, J. K. M. *J. Am. Chem. Soc.* **1990**, *112*, 5525–5534.
- (26) Chakraborty, A.; Deaton, J. C.; Haeefe, A.; Castellano, F. N. *Organometallics* **2013**, *32*, 3819–3829.
- (27) Blanton, C. B.; Murtaza, Z.; Shaver, R. J.; Rillema, D. P. *Inorg. Chem.* **1992**, *31*, 3230–3235.
- (28) Birks, J. B. *Rep. Prog. Phys.* **1975**, *38*, 903–974.
- (29) Kunkely, H.; Vogler, A. *J. Am. Chem. Soc.* **1990**, *112*, 5625–5627.
- (30) Brooks, J.; Babayan, Y.; Lamansky, S.; Djurovich, P. I.; Tsyba, I.; Bau, R.; Thompson, M. E. *Inorg. Chem.* **2002**, *41*, 3055–3066.
- (31) Saito, K.; Nakao, Y.; Sakaki, S. *Inorg. Chem.* **2008**, *47*, 4329–4337.
- (32) Fleetham, T.; Huang, L.; Li, J. *Adv. Funct. Mater.* **2014**, *24*, 6066–6073.
- (33) Adamovich, V.; Brooks, J.; Tamayo, A.; Alexander, A. M.; Djurovich, P. I.; D'Andrade, B. W.; Adachi, C.; Forrest, S. R.; Thompson, M. E. *New J. Chem.* **2002**, *26*, 1171–1178.
- (34) D'Andrade, B. W.; Brooks, J.; Adamovich, V.; Thompson, M. E.; Forrest, S. R. *Adv. Mater.* **2002**, *14*, 1032–1036.
- (35) Kalinowski, J.; Fattori, V.; Cocchi, M.; Williams, J. A. G. *Coord. Chem. Rev.* **2011**, *255*, 2401–2425.
- (36) Strassert, C. A.; Chien, C. H.; Galvez Lopez, M. D.; Kourkoulos, D.; Hertel, D.; Meerholz, K.; De Cola, L. *Angew. Chem., Int. Ed.* **2011**, *50*, 946–950.
- (37) Connick, W. B.; Geiger, D.; Eisenberg, R. *Inorg. Chem.* **1999**, *38*, 3264–3265.
- (38) Hissler, M.; McGarrah, J. E.; Connick, W. B.; Geiger, D. K.; Cummings, S. D.; Eisenberg, R. *Coord. Chem. Rev.* **2000**, *208*, 115–137.
- (39) Lee, J.; Chen, H. F.; Batagoda, T.; Coburn, C.; Djurovich, P. I.; Thompson, M. E.; Forrest, S. R. *Nat. Mater.* **2015**, *15*, 92–98.
- (40) Hanan, E. J.; Chan, B. K.; Estrada, A. A.; Shore, D. G.; Lyssikatos, J. P. *Synlett* **2010**, *2010*, 2759–2764.
- (41) Barone, V.; Cossi, M. *J. Phys. Chem. A* **1998**, *102*, 1995–2001.
- (42) Unger, Y.; Strassner, T.; Lennartz, C. *J. Organomet. Chem.* **2013**, *748*, 63–67.
- (43) Vlček, J. A.; Zláliš, S. *Coord. Chem. Rev.* **2007**, *251*, 258–287.
- (44) Kühn, M.; Weigend, F. *J. Chem. Phys.* **2014**, *141*, 224302–224317.
- (45) Frisch, M. J.; Trucks, G. W.; Schlegel, H. B.; Scuseria, G. E.; Robb, M. A.; Cheeseman, J. R.; Scalmani, G.; Barone, V.; Mennucci, B.; Petersson, G. A.; et al. *Gaussian 09*, revision B.01; Gaussian, Inc.: Wallingford, CT, 2009.
- (46) Hay, P. J.; Wadt, W. R. *J. Chem. Phys.* **1985**, *82*, 299–310.
- (47) Hay, P. J.; Wadt, W. R. *J. Chem. Phys.* **1985**, *82*, 270.
- (48) Yersin, H. *Highly Efficient OLEDs with Phosphorescent Materials*; Wiley: New York, 2008.
- (49) Zhang, C.; Peiju, Y.; Yue, Y.; Xiaojuan, H.; Yang, X. J.; Biao, W. *Synth. Commun.* **2015**, *38*, 2349–2356.
- (50) Lakowicz, J. R. *Principles of fluorescence spectroscopy*; Springer: Berlin, 2006.
- (51) Stephens, P. J.; Devlin, F. J.; Chabalowski, C. F.; Frisch, M. J. *J. Phys. Chem.* **1994**, *98*, 11623–11627.
- (52) Miehlisch, B.; Savin, A.; Stoll, H.; Preuss, H. *Chem. Phys. Lett.* **1989**, *157*, 200–206.
- (53) Becke, A. D. *Phys. Rev. A: At, Mol, Opt. Phys.* **1988**, *38*, 3098–3100.
- (54) Vosko, S. H.; Wilk, L.; Nusair, M. *Can. J. Phys.* **1980**, *58*, 1200–1211.
- (55) Lee, C.; Yang, W.; Parr, R. G. *Phys. Rev. B: Condens. Matter Mater. Phys.* **1988**, *37*, 785–789.
- (56) Rassolov, V. A.; Pople, J. A.; Ratner, M. A.; Windus, T. L. *J. Chem. Phys.* **1998**, *109*, 1223–1229.
- (57) Hehre, W. J.; Ditchfield, R.; Pople, J. A. *J. Chem. Phys.* **1972**, *56*, 2257–2261.
- (58) Hariharan, P. C.; Pople, J. A. *Mol. Phys.* **1974**, *27*, 209–214.
- (59) Hariharan, P. C.; Pople, J. A. *Chem. Phys. Lett.* **1972**, *16*, 217–219.
- (60) Ditchfield, R.; Hehre, W. J.; Pople, J. A. *J. Chem. Phys.* **1971**, *54*, 724–728.
- (61) Hariharan, P. C.; Pople, J. A. *Theoret. Chim. Acta* **1973**, *28*, 213–222.
- (62) Dennington, R. I.; Keith, T.; Millam, J. M.; Eppinnett, W.; Hovell, W. L.; Gilliland, R. *GaussView*, version 3.09; Gaussian Inc.: Wallingford, CT, 2003.